Vibrational dynamics of liquid gallium at 320 and 970 K

L. E. Bove,[1] F. Formisano,[1] F. Sacchetti,[2] C. Petrillo,[2] A. Ivanov,[3] B. Dorner,[3] and F. Barocchi[4]
[1]*INFM, Operative Group Grenoble, F-38042 Grenoble Cedex 09, France*
[2]*INFM and Dipartimento di Fisica, Universitá di Perugia, I-06123 Perugia, Italy*
[3]*Institut Laue Langevin, BP 156, F-38042 Grenoble Cedex 9, France*
[4]*INFM and Dipartimento di Fisica, Universitá di Firenze, I-50019 Firenze, Italy*
(Received 13 August 2004; published 24 January 2005)

The microscopic ion dynamics of liquid gallium was investigated at 320 K—that is, just above the melting point—and 970 K by inelastic neutron scattering experiments and molecular dynamics simulations. The high quality of the experimental data allowed the observation of density fluctuation modes extending up to 1.0 $Å^{-1}$ and existing at both temperatures. At melting, an acousticlike mode propagating with a velocity definitely exceeding the sound velocity was observed, in agreement with the results of a recent inelastic x-ray scattering experiment. The mode velocity and damping were found to be almost temperature independent. The experimental response function was compared with the results of a molecular dynamics simulation, based on a simple model for the effective ion-ion potential which, however, did not contain any temperature-dependent parameter. The result worth noting is that, despite the simple potential, the simulation was capable to reproduce all the observed features of the measured dynamicstructure factor *quantitatively* and at both the temperatures.

DOI: 10.1103/PhysRevB.71.014207 PACS number(s): 61.25.Mv, 78.70.Nx, 71.10.Ay, 61.12.−q

I. INTRODUCTION

One of the most debated and still unsettled subjects of the physics of fluids concerns the microscopic mechanisms responsible for the propagation and the attenuation of density fluctuations in liquid metals. Understanding these mechanisms would enable to distinguish the disorder-driven effects, common to a large class of systems from glasses to undercooled liquids, from those more closely related to the presence of the electron gas and the details of the screened ion-ion potential. Despite several experimental[1–6] and numerical studies[7] of the dynamics of liquid metals, a full understanding of the nature of the collective excitations in the microscopic region, enabling for a unified and sample-independent description, is still missing. The research in this field has been stimulated by the advances in the experimental techniques of inelastic neutron scattering (INS) and inelastic x-ray scattering (IXS), which, being optimally suited to probe the dynamic response at THz frequencies and sub-nm scale, have neatly shown the occurrence of well-defined and long-living acousticlike excitations in the measured spectra of liquid metals. It is now a well-established experimental fact that ion collective modes in liquid metals exist over a wave vector transfer region up to $Q_0/2$, Q_0 marking the position of the first peak of the static structure factor. Recent experiments have also drawn attention to the possible occurrence of more complex time scales associated with the dynamics of liquid metals and driving the decay of the density fluctuations[4–6,8] in the high-frequency regime.

The behavior observed in liquid metals seems to be different from that exhibited by noble gases, where density fluctuations apparently do not propagate for wave vectors Q larger than a small fraction of Q_0, although noble-gas liquids sustain collective modes extending up to $Q_0/2$ (Ref. 9). The experimental evidence in noble gases might be interpreted as an effect brought about by the electron gas which, surrounding the ions in the metal, causes a screening of the long-range ion-ion interactions. The potential role of the electron density and electron gas dynamics in the propagation and damping of the ion density fluctuations in liquid simple metals can be examined by exploiting the simple Bohm-Staver (BS) model for the coupled electron-ion plasma. A discussion of the merits and limitations of this model to describe the whole series of molten alkali metals has been recently presented in Ref. 5. The comparative analysis of Ref. 5 showed the failure of the BS model, when coupled to the long-wavelength random phase approximation (RPA) of the electron dielectric function, in predicting the *absolute* values of the mode velocity for the series of molten alkali metals. The main conclusion was that some beyond-RPA scheme for the dielectric function has to be applied for a proper treatment of the screening effects on the ion density fluctuations. This result, which was stimulated by the search for a common interpretation scheme of the molten alkali-metal series, with a proper account of the electron correlations, goes beyond the excellent quantitative agreement observed in single cases (Na, for example) under the simplified BS approach. On the other hand, the key role of the electron density against ion-core-dependent interactions was emphasized by the success of the scaling relation proposed for the dispersion curves[3] associated with the collective modes of the heavier elements of the alkali-metal series: namely, molten Rb, Cs, and K—Cs alloys. In that case, just the simple BS model was sufficient to provide a meaningful scaling law.

The BS scheme was curiously found to correctly predict the absolute values of the collective mode velocities in liquid Pb (Ref. 2) and Hg (Ref. 4)—that is, in two systems with characteristics profoundly different from the case of molten alkali metals: namely, polyvalent metals with an *sp*-like conduction band, high atomic numbers, and high electron densities. It was not expected that a model like the BS, which reduces the role of the ions to that of pointlike charges, could provide correct mode velocities in a situation of much greater complexity of core repulsive contribution to the in-

teraction potential. Even though a possible explanation of this result could be given by invoking the higher reliability of the RPA prescription, and hence of the BS scheme, in the high-electron-density regime where the kinetic energy dominates over the interaction term in a jellium model, the doubt arises that the agreement observed in Hg and Pb was partly accidental.

To discriminate against the fortuitous agreement arising from balancing effects between the approximated RPA dielectric function and an oversimplified ion-ion interaction and to better define the role of the different contributions to the density fluctuation propagation, a wider class of *sp*-like heavy metals should be investigated. In this paper, we concentrate on liquid gallium as a significant system to distinguish electron screening *versus* core repulsive potential effects in defining the low-momentum ion dynamics in high-electron-density metals. Indeed, liquid Ga has one of the highest ion number densities among the metals belonging to the IIB, IIIA, and IVA groups: namely, $n_i = 0.051$ Å^{-3}. This would correspond to an increased sensitivity to the ion core potential contributions, with respect to Hg ($n_i = 0.039$ Å^{-3}) and Pb ($n_i = 0.033$ Å^{-3}). In addition, the liquid phase of Ga is characterized by an electron density of states approaching that of a nearly-free-electron system,[10] which makes it a good candidate for exploiting the simple model of liquid metal dynamics based on the electron-gas-screened ion-ion interactions.

Over the last years, several experimental investigations have been devoted to the study of structural, electronic, and dynamic properties of liquid gallium.[11–15] While the structure and electronic behavior of this system are consistently defined by a large and substantially coherent body of experimental data, the results about the ion dynamics seem to be rather puzzling. The first INS measurements on liquid gallium[13] at the melting point reported about the nonoccurrence of propagating density fluctuations over the low-wave-vector region, although when fitting the experimental spectra with a damped harmonic oscillator (DHO), heavily damped excitations with frequencies largely above the hydrodynamic values[16] were obtained by the authors. These overdamped collective excitations were associated with high-frequency optical modes that were supposed to contribute to the dynamic structure factor. The absence of acoustic excitations was attributed to the high value of the longitudinal viscosity, thus suggesting a possible anomalous behavior of Ga dynamics in comparison with other liquid metals. Successive INS measurements[14] on liquid gallium at high temperature (970 K) showed the presence of collective excitations at low Q, while two branches, associated by the authors with acoustic and optic modes, were observed at high Q. In disagreement with the results of the INS measurements, a recent IXS experiment[15] carried out on liquid Ga just above the melting point provided a rather neat indication of the presence of acousticlike excitations in the spectra. No evidence for additional optic modes was found over the exchanged wave vector range explored in the IXS experiment, which suggested for molten gallium a behavior similar to that of more common liquid metals.

Considering the relevance of the collective dynamics of liquid Ga in the framework of the RPA treatment of the dielectric function, we believe that the discrepancies between the different experiments deserve clarification. Therefore, we carried out a new INS experiment aiming at obtaining a definite answer about the presence and the nature of collective modes in liquid Ga and their evolution with the temperature. We investigated the low-Q dynamics of liquid gallium at 320 K to make a comparison with the previous INS (Ref. 13) and IXS (Ref. 15) data and at 970 K to study the temperature dependence without changing the instrument configuration and to compare with the data of Ref. 14. We exploited the combination of small angle and high incoming neutron energy, offered by the present top-performance three-axis neutron spectrometers, to extend the accessible dynamic range while pushing the energy resolution of the instrument to its maximum. These favorable conditions enabled us to make a quantitative and accurate comparison between neutron and x-ray results. The description of the low-momentum, high-energy liquid gallium dynamics was complemented by an extended large-scale molecular dynamics (MD) simulation applied to the calculation of both the coherent and incoherent contributions to the dynamic structure factor. The simulation was based on a simple phenomenological model for the ion-ion potential, which we developed in the framework of the two-component model to describe liquid polyvalent metals.[8]

II. EXPERIMENT

The neutron measurements were carried out at the three-axis spectrometer IN1 installed at the High Flux Reactor of the Institut Laue Langevin (ILL, Grenoble, France). The experimental setup was carefully chosen to optimize the resolution versus the dynamic range. The optimal experimental conditions were identified according to the experience gained in similar experimental investigations.[17] In order to obtain high-energy resolution and to access to as low as possible scattering angles, Soller collimators providing 25′, 20′, 20′, and 30′ collimations were mounted on the neutron path from the reactor to the detector. A vertically focusing Cu(331) monochromator was employed, coupled to a vertically focusing Cu(400) analyzer set at a fixed final wave vector equal to 7.0 Å^{-1}. A vacuum box, 1 m in diameter, was also installed at the sample position to reduce the air scattering and thus the background. By this spectrometer configuration, high-quality data were collected down to 1° scattering angle. Despite the tight collimations, the high flux of the neutron source, fully exploited thanks to the large-area monochromator and analyzer crystals, ensured enough intensity available at the sample position.

The sample was 99.999%-pure gallium with natural isotopic composition, 80 g mass, contained inside a flat 70 mm × 35 mm × 10 mm molybdenum cell with 0.5 mm wall thickness. The measurements were carried out at two temperatures: namely, 320 K and 970 K. A standard ILL furnace was used for the high-temperature measurements, while a system of four resistive elements, mounted at the top and bottom edges of the cell, was operated in conjunction with a standard ILL temperature controller for the low-temperature experiment. The intensity scattered from the sample was measured at five wave vector transfer values Q: namely, Q

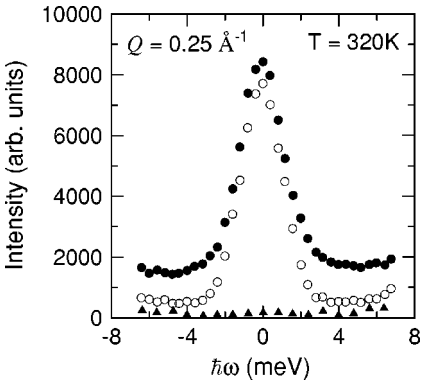

FIG. 1. Raw intensity versus energy transfer as measured at $T=320$ K and wave vector transfer $Q=0.25$ Å^{-1} on molten gallium (dots), empty molybdenum cell (circles), and full absorbing cadmium (triangles).

$=0.25$, 0.3, 0.4, 0.7, and 1.0 Å^{-1}. The background from the empty molybdenum cell was measured in the same conditions as the sample, while the background produced outside the sample region was measured at $Q=0.25$, 0.3, and 0.7 Å^{-1} by shielding the cell with a 1-mm-thick highly absorbing Cd plate at 320 K and a B_4C plate at 970 K. Additional background measurements were carried out removing the cell, with the furnace in place and without the furnace, and collecting data along inelastic scans at the same Q values as the sample. As an example, the intensities measured from the sample, the empty cell, and the cadmium absorber at $Q=0.25$ Å^{-1} and $T=320$ K are shown in Fig. 1. The contribution of the molybdenum cell was dominated by the central peak, originating from elastic processes, with tails of low intensity. The instrument background contribution was very low as shown by the data of the absorbing plate. A quite similar, very low, background was found to affect the high-temperature measurements. To check for the resulting energy resolution of the instrument, a scan at $Q=0.3$ Å^{-1} was carried out by inserting a 1.5-mm-thick vanadium plate inside the sample cell. The experimental elastic resolution function was found to be well modeled by a Gaussian function with 2.4 meV full width at half maximum (FWHM), in very good agreement with the resolution function calculated according to Ref. 18 for the known spectrometer configuration and parameters. The sample transmission was obtained by a direct measurement of the intensity transmitted throughout the molybdenum cell, either empty or filled with the sample. For these measurements the incoming beam intensity was reduced by inserting an attenuator along the primary neutron path. The measured values of the transmission—namely, $T=0.665$ at 320 K and $T=0.643$ at 970 K—were found to be in good agreement with the estimates based on the tabulated values of the coherent and incoherent scattering cross sections and spin-dependent neutron scattering lengths.[19]

The data reduction was performed following the well-assessed procedure,[20] successfully applied in similar investigations.[3–5,17] The single-scattering intensity from the sample was obtained by subtracting the multiple-scattering (MS) contribution from the background- and monitor-corrected data. The correction for the MS contribution is a

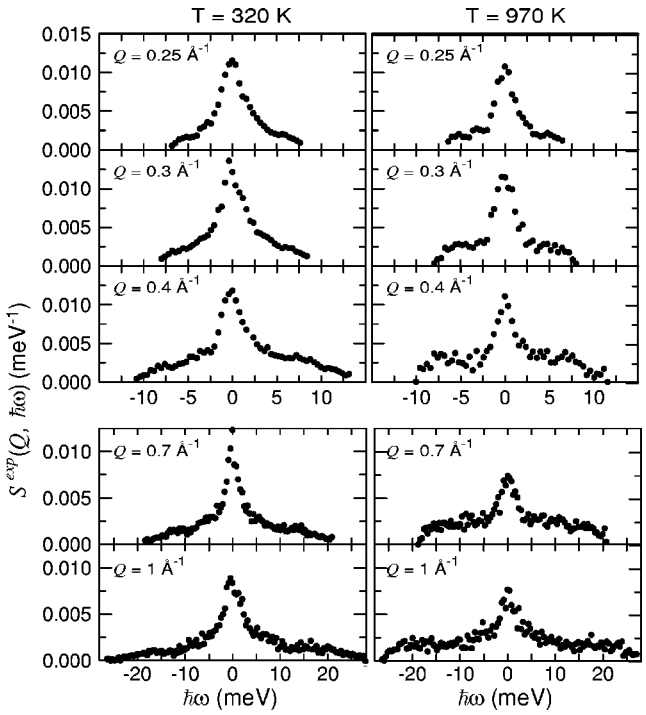

FIG. 2. Experimental dynamic structure factor $S^{expt}(Q,\hbar\omega)$ of molten gallium at 320 K and 970 K versus energy transfer and at the wave vector transfer values of the measurements.

critical step of the data reduction. Indeed, even though the present sample is a fairly weak scatterer, the MS contribution is comparable with that of single-scattering events at low wave vectors. This is a consequence of the small values attained by the static structure factor $S(Q)$ over the low-Q range [$S(0)=0.006$ at 320 K], against MS, which gets in contributions from processes at every Q value. To the purpose of calculating the MS contribution with the high accuracy needed in the present experimental conditions, a detailed knowledge of the sample scattering function over a wide energy and momentum range is required *a priori*. With the lack of experimental data, we used the dynamic structure factor of liquid Ga obtained from the molecular dynamics simulations, described in the next section, as the input model for the MS correction. Indeed, the MD simulation provided a calculated dynamic structure factor over a wide wave vector and energy transfer range: namely, $0.05\leqslant Q\leqslant 15$ Å^{-1} and $-30\leqslant\hbar\omega\leqslant 30$ meV.

From the MS-, background-, and attenuation-corrected sample intensities, the experimental dynamic structure factor $S^{expt}(Q,\hbar\omega)$, which contains both the coherent and incoherent contributions, was obtained. The data at the two temperatures are shown in Fig. 2 at the Q values of the experiment and as a function of the energy transfer. As apparent from Fig. 2, side peaks originating from inelastic (Brillouin) scattering can be observed up to the maximum investigated Q values at both temperatures, which indicates the presence of collective modes in the spectra. It is worth noting that, although the incoherent term dominates the scattering cross section at low-wave-vector transfers Q, its contribution ($\sim 80\%$) to the experimental $S^{expt}(Q,\hbar\omega)$ concentrates below the quasielastic peak, which enables the side structures

of the collective modes to be unambiguously detected. Increasing Q the inelastic peak position shifts towards higher energies with a propagation velocity of the order of 20 meV Å (about 3100 ms^{-1}) at 320 K. This rough estimate provides a value in qualitative agreement with that reported in the recent IXS experiment[15] and in excess of the sound velocity as measured at the same temperature by ultrasound spectroscopy[16]—that is, 2780 ms^{-1}. It is also interesting to observe that the Brillouin light scattering experiment of Ref. 21 provided quite a large value for the mode velocity, although, because of the severe limitations of this technique in the case of metals, the results could be affected by surface effects. At high temperature, the inelastic structures of the neutron spectra appear at slightly lower energy and seem to be better defined. At both temperatures and for all the wave vector transfer values, a broad quasielastic signal, superimposed onto the sharp diffusion-related central peak, is apparent in the data. The width associated with this quasielastic contribution clearly exceeds the instrument resolution function, with effects on the visibility of the collective modes which cannot be ruled out.

III. MD SIMULATION

MD simulations of liquid gallium, based on a numerical potential extracted from the measured diffraction data[11] by using the predictor-corrector procedure, were carried out by Bermejo *et al.*,[13] in order to get additional data on the apparently unusual gallium dynamics. However, while the agreement between simulated and experimental static structure factors was excellent, as expected for a potential derived by an inversion method, the collective dynamic behavior was poorly described. More recently, first-principles simulations have been applied to the description of the electronic configuration and the static structure of liquid gallium.[10] In that work the ion-ion interaction was evaluated self-consistently from the electron states by means of a finite-temperature local density functional approach. Unfortunately, severe computing time limitations prevent the application of this method to probing the dynamic correlation functions over both long times, up to several ns, and low Q, over the nm^{-1} region, as required by the present case.

We carried out standard constant density classical MD simulations of liquid gallium using a system of 87 808 particles for a total simulation time of 2 ns in steps of 0.2 fs. A cubic box with periodic boundary conditions and a leapfrog algorithm to integrate the equation of motion were employed. The force cutoff distance was 10.5 Å. The box edge was fixed according to the density and it was equal to 118.8 Å at $T=320$ K and 121.46 Å at $T=970$ K. The minimum value of the useful wave vector in the simulation was ~ 0.05 $Å^{-1}$, which was small enough for a safe comparison with the experimental data. The simulation was based on a simple analytic potential to model the ion-ion interactions in liquid gallium. The proposed model potential had been previously tested in the case of liquid mercury and found to reproduce the static properties with very high accuracy.[8] The pair potential was given by

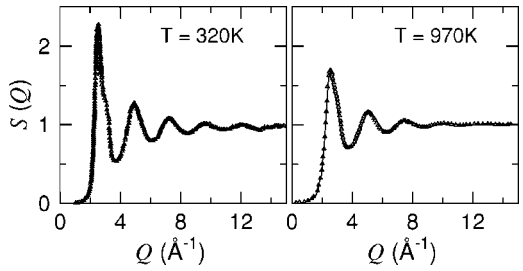

FIG. 3. Static structure factor $S(Q)$ of liquid Ga at 320 K and 970 K, as obtained from present MD simulations (solid line) in comparison with the experimental data from Ref. 11 (open triangles).

$$V(r) = \frac{V_R}{r^{12}} + V_F \frac{\cos(2k_F r + \phi)}{r^3} \exp(-k_{TF} r), \qquad (1)$$

where r is the ion-ion distance, $2k_F$ is the diameter of the Fermi sphere, and k_{TF} is the Thomas-Fermi wave vector. V_R, V_F, and ϕ are parameters to be determined. The basic assumption beneath this representation of the potential is that the interaction in *sp*-like polyvalent metals can be adequately described by taking the sum of a long- and a short-range part. The short-range part, which represents the repulsive interaction due to the overlap of the electron cores, was simply modeled by an inverse power law, with the same exponent as the Lennard-Jones potential. The long-range part was taken as the asymptotic form of the effective ion-ion interaction, screened by the conduction electrons[22] as modeled by an almost uniform electron gas. A number of electrons per atom equal to $Z=2.7$, the effective ionic charge from which to evaluate the electron number density, and hence k_F and k_{TF}, was assumed according to the scheme proposed in Ref. 10 to obtain the number of *sp*-like electrons. The parameters V_R, V_F, and ϕ were optimized by fitting the simulated static structure factor $S(Q)$, which was directly calculated as the Fourier transform of the pair correlation function $g(r)$, to the experimental data[11] measured at 320 K, and corresponding to a mass density $\rho=5.904$ g cm^{-3}. The same set of parameters for the potential was used for the simulation at 970 K, while the mass density was lowered to $\rho=5.674$ g cm^{-3} and k_F and k_{TF} were scaled according to the density change.

The energy conservation, at both temperatures, was as good as a few parts in 10^{-4}. By slowly cooling the system, we found a crystallization temperature equal to 307 K, which compares rather well with the experimental melting temperature—i.e., 303 K. The simulated system crystallizes in a structure compatible with the stable phase α-Ga—i.e., a base-centered orthorhombic lattice with eight atoms per unit cell. When rapidly decreasing the temperature of the simulated liquid below the melting point, we obtained a supercooled liquid down to 190 K. We did not check the melting of the crystal because of the very long simulation runs necessary to do it.

Figure 3 shows the simulated static structure factors $S(Q)$ at the two temperatures of this experiment, in comparison with the neutron diffraction data of Ref. 11. The agreement between the two sets of data is impressively good, as appar-

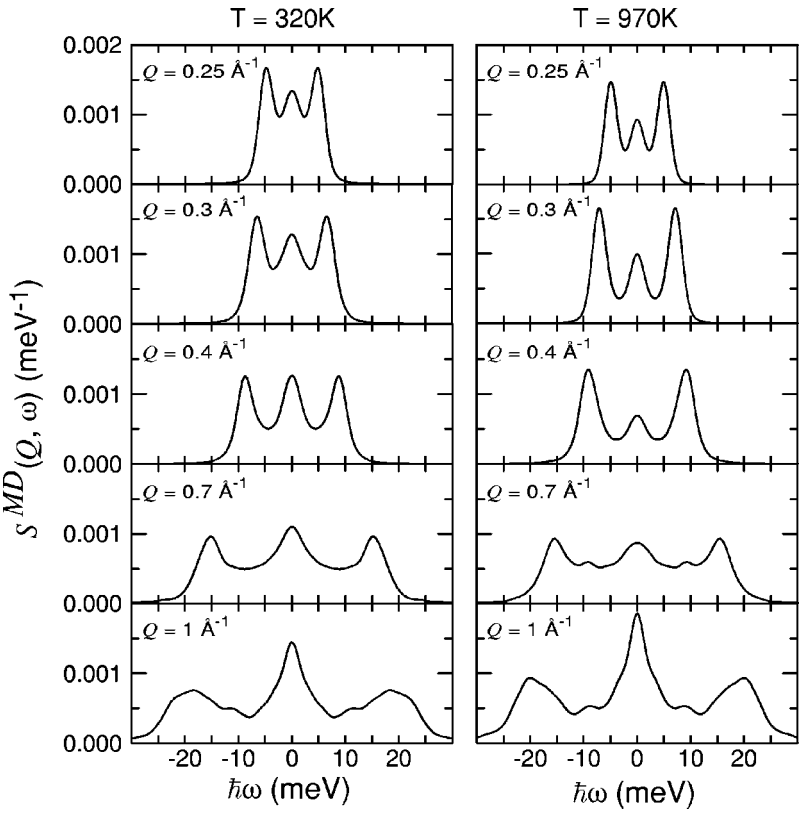

FIG. 4. Simulated dynamic structure factor $S^{MD}(Q,\omega)$ of molten gallium at 320 K and 970 K versus energy transfer and at the wave vector transfer values of the measurements. The curves here shown are after convolution of the MD results with the INS experimental resolution.

ent from Fig. 3. In particular, we remark that the shape of the first peak, the period, and the amplitude of the oscillation are well reproduced, as well as the asymmetry of the first diffraction peak of the liquid. This specific feature is related to the interplay between the two different length scales associated with the diameter of the repulsive core and with the wavelength $\lambda_F = \pi/k_F$ of the Friedel oscillation, respectively. The good agreement at high temperature is a remarkable fact since, as already observed, the fitting parameters V_R, V_F, and ϕ were fixed by adjusting them at 320 K only, and the density dependence of the potential was entirely described by the change of the electron density. This result points out that the electron density correctly accounts for the presence of many-atom contributions to the effective pair potential in liquid gallium.

The MD simulation was applied to inspect a selection of the dynamic properties of the system. In particular, we calculated the time-dependent mean-square displacement $\langle[\Delta r(t)]^2\rangle$ by averaging over all the atoms in the system. In such a way, we obtained the long-time limit of $\langle[\Delta r(t)]^2\rangle$: namely, $6D|t|$, where D is the diffusion coefficient. Diffusion coefficient values equal to 1.5×10^{-5} cm^2 s^{-1} at 320 K and to 1.3×10^{-4} cm^2 s^{-1} at 970 K were obtained, again in excellent agreement with the corresponding experimental data[23]—that is, 1.57×10^{-5} cm^2 s^{-1} at 320 K and 1.31×10^{-4} cm^2 s^{-1} at 970 K.

To investigate the propagation of the ion density fluctuations in liquid gallium, we calculated the intermediate scattering function $F(Q,t)$ defined as

$$F(Q,t) = \langle \rho(Q,t-t')\rho(Q,t')\rangle,$$

where $\rho(\boldsymbol{Q}) = N^{-1/2}\Sigma_j \exp[-i\boldsymbol{Q}\cdot\boldsymbol{r}_j(t)]$ is the Fourier component of the atomic density at the wave vector $\boldsymbol{Q}$ and $\boldsymbol{r}_j(t)$ is the trajectory of the jth particle. $F(Q,t)$ was computed directly from its defining equation by averaging over the time t' and the orientation of $\boldsymbol{Q}$. As known, the Fourier transform of $F(Q,t)$ is the dynamic structure factor $S^{MD}(Q,\omega)$ of the system, which can be easily compared with what is measured in inelastic neutron or x-ray scattering experiments. $S^{MD}(Q,\omega)$ was obtained from the power spectrum of the density fluctuations by applying the Welch method,[24] and it was calculated for Q ranging from 0.1 to 1.5 Å^{-1} by taking the average over all possible $\boldsymbol{Q}$ orientations. Each $S^{MD}(Q,\omega)$ at fixed constant Q was obtained as an average over different statistically independent runs.

The dynamic structure factor $S^{MD}(Q,\omega)$ is shown in Fig. 4 at the Q values and the two temperatures of the experiment, after convolution of the data with the four-dimensional $(\boldsymbol{Q},\omega)$-dependent resolution function of the spectrometer. Collective excitations, characterized by a damping-to-frequency ratio smaller than unity, are visible at both temperatures, and they are superimposed to a broad quasielastic contribution. We remark that, for an effective and quantitative use of $S^{MD}(Q,\omega)$ for MS subtraction from the measured neutron data, both the calculated dynamic structure factor $S^{MD}(Q,\omega)$ and its self-part are necessary. Indeed, as discussed at the end of Sec. II, the dynamic structure factor which is probed in the neutron experiment consists of a coherent and an incoherent contribution and it has to be compared with the (coherent and incoherent) cross-section-weighted sum of $S^{MD}(Q,\omega)$ and its self-term. This is not the case for $S^{expt}(Q,\hbar\omega)$ measured in the inelastic x-ray scattering experiment, which is intrinsically coherent and can be compared directly with the (coherent) cross-section-weighted $S^{MD}(Q,\omega)$.

IV. DATA ANALYSIS AND DISCUSSION

To disclose the essential features of the system dynamics contained in the experimental $S^{expt}(Q,\hbar\omega)$ data, we preferred to carry out an MD-independent analysis based on a simple empirical fit of the data, instead of using the simulated $S^{MD}(Q,\omega)$ as a model fitting function. This procedure amounts to treating the experimental and simulated data as two independent sets of data.

The first choice for the model fitting function was given by the superposition of a DHO, modeling the purely inelastic component $S_{inel}(Q,\omega)$, and a single Lorentzian function, describing the quasielastic contribution $S_{qe}(Q,\omega)$. As already observed in other liquid metals,[4,5] this very basic model did not provide high-quality fits to the data in the quasielastic region. However, differently from the other liquid metals where the inadequacy of modeling the quasielastic contribution by a single Lorentzian seemed just a fitting problem, in the case of liquid gallium this finding is convincingly supported by the results of the MD simulation. Indeed, a thorough analysis of the self-intermediate scattering function as obtained from the simulation showed that at least two main contributions, associated with two different time scales, characterize the self-dynamics of liquid gallium.[25] The slower process was seemingly associated with the usual diffusion while the faster one was related to the residence time of the particle within the cage of its first neighbors. According to the MD simulations,[25] the time scale associated with the fast and Q-independent process was characterized by the values $\tau_0^{MD}=0.22$ ps at 320 K and $\tau_0^{MD}=0.13$ ps at 970 K. In the energy domain, the fast process gives rise to an additional Lorentzian function, besides the diffusive one, with associated FWHM values[25] equal to 6.9 meV at 320 K and 11.7 meV at 970 K. These values are consistent with the size of the width of the broad quasielastic structure, visible in the experimental data beneath the narrow diffusive contribution. For these reasons, we believe that a two-Lorentzian function model would give a more appropriate description of the experimental quasielastic structure, which appears as a superposition of a narrow and a broad component. Therefore, the dynamic structure factor was modeled by the sum of $S_{qe}(Q,\omega)$ and $S_{inel}(Q,\omega)$ where

$$S_{qe}(Q,\omega)=\frac{\hbar\omega/k_BT}{1-\exp(-\hbar\omega/k_BT)}\left[\frac{a_0(Q)}{\pi}\frac{\Gamma_0(Q)}{\omega^2+\Gamma_0^2(Q)}+\frac{a_1(Q)}{\pi}\frac{\Gamma_1(Q)}{\omega^2+\Gamma_1^2(Q)}\right], \tag{2a}$$

$$S_{inel}(Q,\omega)=[n(\omega)+1]a_c(Q)\frac{\Gamma_c(Q,\omega)}{[\omega^2-\omega_c^2(Q)]^2+\Gamma_c^2(Q,\omega)}, \tag{2b}$$

$n(\omega)$ being the Bose factor. The convolution of this model dynamic structure factor with the four-dimensional $(\boldsymbol{Q},\omega)$-dependent resolution function was fitted to the experimental $S^{expt}(Q,\hbar\omega)$. In principle, the free parameters of the fit were the three amplitudes $a_0(Q)$, $a_1(Q)$, and $a_c(Q)$, the three widths $\Gamma_0(Q)$, $\Gamma_1(Q)$, and $\Gamma_c(Q,\omega)$, and the frequency $\omega_c(Q)$. However, the number of parameters was effectively reduced by assuming, for the width of the narrow quasielastic Lorentzian, the expression

$$\Gamma_0(Q)=\frac{DQ^2}{1+\tau_0DQ^2},$$

with the diffusion coefficient D equal to the experimental data[23] and τ_0—i.e., the residence time for a random-jump diffusion model, given by the MD values calculated at the two temperatures. Moreover, the ω dependence of the damping factor $\Gamma_c(Q,\omega)$ was approximated[26] by the linear function $\Gamma_c(Q,\omega)=\omega\Gamma_c(Q)$, with $\Gamma_c(Q)$ the effective parameter. The width $\Gamma_1(Q)$ associated with the broad Lorentzian was found to be almost Q independent, and hence it was held constant during the fitting procedure. An example of the results obtained from the fitting procedure is presented in Fig. 5, where best-fitting curves and experimental data at $Q=0.3$ Å^{-1} are compared. The broad quasielastic component and the inelastic contribution are also shown. The good quality of the fit indicates that the model function correctly reproduces the important features of the experimental data. We observe that the best-fit values of Γ_1 turned out to be $\hbar\Gamma_1=6.7\pm0.4$ meV at 320 K and $\hbar\Gamma_1=11.2\pm0.4$ meV at 970 K, with $1/\Gamma_1$ in strikingly good agreement with the fast relaxation time values τ_0^{MD} provided by the MD simulations.

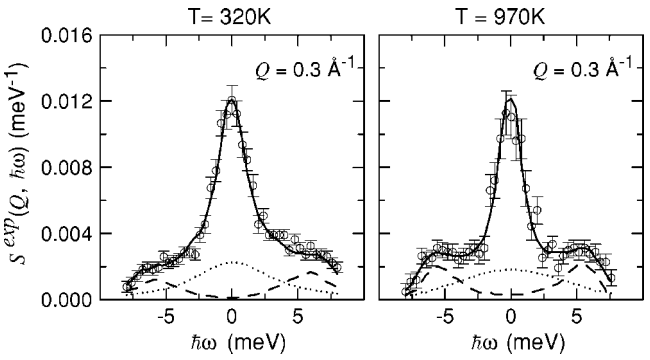

FIG. 5. $S^{expt}(Q,\hbar\omega)$ of molten gallium at 320 K and 970 K versus energy transfer and at the wave vector transfer $Q=0.3$ Å^{-1} (circles). The solid lines are the curves calculated according to the fitting model described in the text. The dashed line is the inelastic contribution (DHO) and the dotted line the fast quasielastic process.

For a meaningful comparison of the purely inelastic features contained in $S^{expt}(Q,\hbar\omega)$ and $S^{MD}(Q,\omega)$, the two sets of data had to be treated using the same empirical model; that is, the dynamic structure factor $S^{MD}(Q,\omega)$, after convolution with the resolution function and the trivial normalization to the integrated intensity, was fitted using the model functions given in Eqs. (2). The dispersion curve associated with the collective modes and defined by the fitting parameter $\omega_c(Q)$ for both the experiment and the MD simulation is shown in Fig. 6. The same empirical approach was applied to analyze the recent IXS data[15] at 315 K and the dispersion curve resulting from the fitting procedure is also shown in Fig. 6. This figure emphasizes the agreement, within the experimental errors, of the three dispersion curves obtained with the three different techniques.

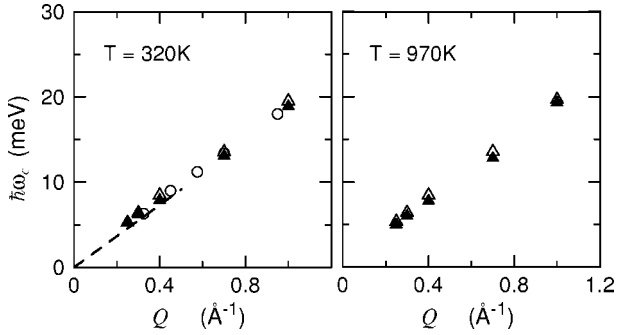

FIG. 6. Dispersion relation $\hbar\omega_c(Q)$ versus Q at 320 K and 970 K, as obtained from the present fitting model: present neutron data (solid triangles), MD simulations (open triangles), and x-ray data at melting (circles) from Ref. 15. Error bars are within the symbol size. The dashed line is the sound dispersion.

In Fig. 7 the damping factor $\Gamma_c(Q)/Q$ is compared with the companion data obtained by fitting the MD simulation data [Eq. (2)]. The two sets of data are, once again, in good agreement among each other and both are consistent with the approximation $\Gamma_c(Q) \sim \gamma_d Q$, where γ_d is a Q-independent constant. This expression for $\Gamma_c(Q)$ is consistent with the RPA treatment of the dynamic structure factor of a liquid metal when described as the two-component plasma of interacting electrons and ions.[26] We remark that the mode damping appears to be of comparable size at the two temperatures. Hence, the better visibility of the modes at high temperature is more likely due to the broadening of the quasielastic contribution, which becomes an almost flat background at 970 K over the present energy range. Our results at 320 K suggest that the failure in observing the collective modes, as reported in Ref. 13, was probably due to the limited dynamic range of the experiment.

It is also interesting to evaluate the ratio of the bulk, η_B, to shear, η_S, viscosities given by the following relationship:[27]

$$\frac{\eta_B}{\eta_S} = \frac{5}{3}\frac{\int_0^\infty drr^2 g(r)[V''(r) + V'(r)/r]}{\int_0^\infty drr^2 g(r)[V''(r) + 4V'(r)/r]},$$

where $V'(r)$ and $V''(r)$ are the first and second derivatives of the potential and $g(r)$ is the measured pair-correlation

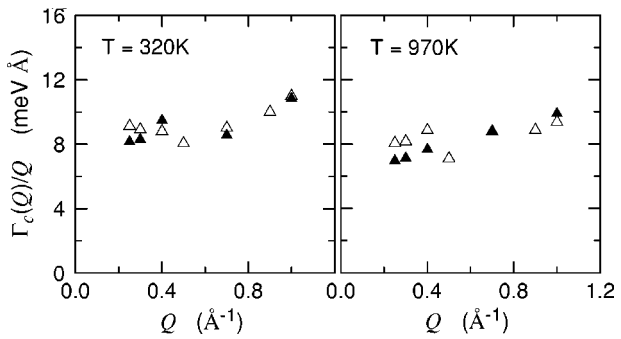

FIG. 7. $\Gamma_c(Q)/Q$ versus Q. Present neutron data (solid triangles) and MD simulations (open triangles).

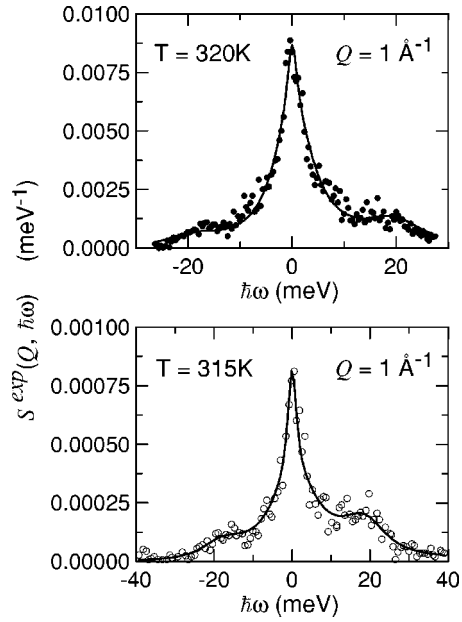

FIG. 8. Comparison between experimental (neutron, dots; x-ray, circles) and simulated (solid line) dynamic structure factor of liquid gallium at 320 K and at the wave vector transfer $Q=1$ Å^{-1}. The present neutron data are compared with the simulated *total* dynamic structure factor, after convolution with the INS experimental resolution. The x-ray data from Ref. 15 are compared with the simulated coherent contribution only, after convolution with the IXS experimental resolution function.

function.[11] Applying this equation to the model potential given in Eq. (1), we obtained η_B/η_S equal to 4.8 at 320 K and to 3.2 at 970 K. Making use of the experimental data of the shear viscosity, after Ref. 13, the corresponding values of the hydrodynamic limit of the longitudinal viscosity can be obtained from the quoted ratios. It was found $\eta_B=11.3$ cP at 320 K, in very good agreement with the estimate provided by the IXS experiment,[15] and 9.9 cP at 970 K. These results suggest that there is only a small effect of the viscosity on the collective mode propagation.

In an attempt of further reducing the number of free parameters and simplifying the fit, we exploited the feature of $\omega_c(Q)$ being almost linear up to $Q=0.5$ Å^{-1}, as apparent from Fig. 6. The fit was then repeated with Γ_1 constant and $\omega_c(Q)=c_0 \sin(\pi Q/Q_0)$, c_0 being the collective mode velocity and Q_0 the position of the first maximum in the static structure factor. The final fitting scheme was therefore one comprising the simplified damping factor $\Gamma_c(Q)$, the two Q-independent parameters Γ_1 and c_0, and the three linear fitting parameters: namely, the amplitudes $a_0(Q)$, $a_1(Q)$, and $a_c(Q)$. The collective mode velocity turned out to be $c_0 = 3080 \pm 180$ m s^{-1} at $T=320$ K and $c_0=3020\pm200$ m s^{-1} at $T=970$ K. As already observed, the value of c_0 at 320 K is in good agreement with that measured in the IXS experiment[15] and larger than the sound velocity[16] (2780 m s^{-1}), consistently with what found in many other liquid metals.[6]

Finally, in Fig. 8 the dynamic structure factor calculated by the MD simulation at 320 K and $Q=1$ Å^{-1} is shown in comparison with the experimental neutron and x-ray dynamic structure factors. In particular, the simulated neutron

TABLE I. Velocity associated to the collective mode in molten alkali and polyvalent metals. c_{expt}, as observed in neutron and x-ray scattering experiments; c_{BS}^{RPA}, calculated under the BS scheme with the RPA prescription for $\epsilon(Q)$; c_{BS}^{LF}, calculated under the BS scheme with local field included. Note the imaginary value of c_{BS}^{LF} in liquid cesium. The quantity $[R^2/6+D_p]$ accounts for the ion size contribution (see text). Z is the effective number of conduction electrons.

	Z	r_s	c_{expt} (meV Å)	c_{BS}^{RPA} (meV Å)	c_{BS}^{LF} (meV Å)	$[R^2/6+D_p]$ (Å^2)
Li	1.00	3.303	36.5	42.80	27.51	0.12 ± 0.02
Na	1.00	4.053	18.5	19.16	9.98	0.31 ± 0.05
K	1.00	5.021	15.5	11.86	3.46	0.93 ± 0.13
Rb	1.00	5.355	9.2	7.52	1.07	0.91 ± 0.10
$K_{52}Cs_{48}$	1.00	5.41	11.2	8.95	0.87	0.97 ± 0.12
Cs	1020	5.776	7.5	5.59	$1.40i$	1.14 ± 0.13
Ga	2.70	2.430	20.3	30.16	22.86	-0.03 ± 0.02
Ge	2.00	2.630	20.5	23.50	17.24	0.07 ± 0.02
Sn	2.00	2.810	19.0	17.20	12.22	0.23 ± 0.04
Hg	2.00	2.700	13.8	13.77	9.98	0.15 ± 0.03
Pb	1.87	2.970	11.4	11.91	8.21	0.15 ± 0.04

response function contains both the dynamic structure factor and the self-dynamic structure factor for a proper account of the coherent and incoherent contributions to the neutron spectra. For the comparison with the IXS spectra of Ref. 15, only the purely coherent component was considered. As apparent in Fig. 8, the MD simulations provide an excellent quantitative account for the experimental results of both INS and IXS measurements.

V. CONCLUDING REMARKS

As described in the previous sections, it is now well established that liquid gallium sustains well-defined collective modes up to wave vector transfer values $Q=1$ Å^{-1}, both at melting (320 K) and at high temperature (970 K), with associated velocities equal to 3080 ± 100 m s^{-1} and 3020 ± 100 m s^{-1}, respectively. Both the propagation velocity and the damping of the modes are scarcely temperature dependent.

The Bohm-Staver estimate for the sound velocity, calculated using the RPA approximation for the electron dielectric function and assuming a number of electrons per atom equal to 2.7 according to Ref. 10, returns the value 4600 m s^{-1}, which is largely in excess of the experimental one. This is an unambiguous indication that the simple model of pointlike ions embedded in an RPA-treated electron gas is not adequate to quantitatively describe the dynamics of liquid gallium. On the other hand, the experimental observation that the collective mode velocity does not depend on temperature is consistent with what expected from the BS formula, which suggests 1.027 as velocity ratio at the two temperatures as a consequence of the small density change between 320 K and 970 K. Moreover, we found that the present MD simulation relying on an electron-gas-based model potential is quite effective in reproducing the experimental data. In the model potential an equally important role is played by both the repulsive component, coming from the ion core contribution, and the Friedel-like oscillations, originating from the electron gas screening. In fact, both static and dynamic properties of gallium cannot be reproduced by the empty-core pseudopotential, which works correctly in the case of alkali metals. It is important to note that the model potential we used is not a purely two-body interaction. Indeed, the many-body effects are contained into the electron-density-dependent parameters k_F and k_{TF}. Therefore, the capability of this potential to reproduce quantitatively several static and dynamic properties of liquid gallium underlines the fundamental role of the electron gas in the system.

As mentioned in the introductory section, the BS approximation, although failing in predicting the quantitatively correct values of the mode propagation velocity for the whole class of alkali metals,[5] surprisingly provides good estimates in the case of Hg (Ref. 4) and Pb (Ref. 2). It is also interesting to observe that BS estimates of the collective-mode velocities in liquid Sn and Ge, the latter being metallic in the liquid phase, are in satisfactory agreement with the experimental values provided by the IXS experiments in Sn (Ref. 28) and Ge (Ref. 29). However, if the successful BS prediction were brought about by the rather high electron density of these metals, an even more accurate prediction is to be due for the higher-electron-density gallium. On the contrary, the evidence of a substantial disagreement between BS and experimental values of the velocity points out that some compensation between electron-driven interactions and the finite size of the ion core must occur.

A quantitative overview of the situation in alkali and heavier *sp*-like metals is presented in Table I, where the experimental data of the collective-mode velocity are compared with the results of calculations carried out in the realm of the BS model, with both RPA and beyond-RPA treatments of the electron dielectric function. The main improvement over the BS model, which consists in restoring the finite size of the ions, was also treated and the results are reported in Table I.

The main steps of the present analysis are summarized in the following.

The interpretation of the experimental collective-mode dispersion exploits the equations of motion for the homogeneous and interacting *electron-phonon* system.[30] A self-consistent treatment of the system coupled-dynamics accounts for the mutually induced effects between the phonon field, associated with the ions, and the electron cloud. The renormalized phonon dispersion relation, which is adopted to describe the ion-density fluctuations in the liquid metals, is

$$\omega^2(Q) = \Omega_{ion}^2(Q) - \frac{Q^2}{4\pi e^2}|v(Q)|^2\left[1 - \frac{1}{\epsilon(Q)}\right], \qquad (3)$$

where $|v(Q)|$ is the coupling coefficient between the vibrational field of the ions and the electron distribution, and $\Omega_{ion}^2(Q)$ is the bare frequency of the ion collective mode. The static approximation for the dielectric function $\epsilon(Q)$ is appropriate to treat the ion dynamics, which is slow on the scale of the electron motions.

The BS model is easily obtained from Eq. (3) as the long-wavelength limit dispersion of the ionic plasma—that is, the homogeneous system of pointlike ions and electrons coupled through purely Coulombic interactions.[30] The bare frequency reduces to the Q-independent plasma frequency of the ions, Ω_p, as it does the coupling term $Q^2|v(Q)|^2/4\pi e^2$, which results in the known dispersion relation $\omega_{BS}^2(Q) = \Omega_p^2/\epsilon(Q)$. Making use of the definition

$$\frac{k_s^2}{Q^2 + k_s^2} = \frac{\epsilon(Q) - 1}{\epsilon(Q)},$$

which introduces the virtually exact screening wave vector k_s, the long-wavelength limit of the BS dispersion relation can be written as

$$\lim_{Q\to 0} \omega_{BS}^2(Q) = \frac{Q^2\Omega_p^2}{k_s^2},$$

with the associated velocity of the ion-density fluctuations:

$$c_{BS} = \lim_{Q\to 0}\frac{\omega_{BS}(Q)}{Q} = \frac{\Omega_p}{k_s}.$$

Under the RPA prescription for the long-wavelength limit of $\epsilon(Q)$, k_s would be coincident with the Thomas-Fermi wave vector k_{TF}. The velocity values calculated according to this approximation are listed in Table I, under the column heading c_{BS}^{RPA}.

An improved beyond-RPA scheme includes the local field effects into the dielectric function, which can be easily accomplished through the exact screening wave vector k_s—that is,

$$k_s^2 = \frac{k_{TF}^2}{1 - \lambda k_{TF}^2},$$

where the low-Q, zero-frequency local field coefficient λ is related to the correlation energy per particle of the electron gas, ϵ_c, through the compressibility sum rule[31]

$$\lambda = \frac{1}{4k_F^2}\left(1 + \frac{\pi}{3}\alpha r_s^2\frac{\partial\epsilon_c}{\partial r_s} - \frac{\pi}{6}\alpha r_s^3\frac{\partial^2\epsilon_c}{\partial r_s^2}\right),$$

with $\alpha = (4/9\pi)^{1/3}$, and the dimensionless parameter r_s defined through $1/n = \frac{4}{3}\pi r_s^3 a_0^3$, n the electron number density, and a_0 the Bohr radius. Quite reliable estimates of ϵ_c are nowadays provided by interpolation schemes based on quantum Monte Carlo simulations. Exploiting one of these schemes,[32] the known instability of the electron gas at low densities, was observed at the cutting value $r_s = 5.5$, above which the electron gas compressibility and k_s^2 take negative values. As a consequence, the collective modes of the pointlike ions cannot propagate for $r_s \geqslant 5.5$. The values of the velocities resulting from this calculation are reported in Table I under the column heading c_{BS}^{LF}.

Considering that the stability of real systems, including heavy alkali metals, is not affected by them attaining r_s values close to or even beyond the calculated threshold, the role played by the ion finite size on the metal stability is crucial, especially for the low-electron-density systems. The effects of the finite size of the ion core on the collective-mode dispersion in the low-Q limit can be investigated by leaving aside the BS model, independently of the scheme used for $\epsilon(Q)$, and turning back to the general equation (3). A simple approximation to this equation, which reproduces the correct long-wavelength behavior of the dispersion relation and accounts for the internal structure of the ions, consists in keeping the low-Q expressions[33]

$$\Omega_{ion}^2(Q) \sim \Omega_p^2(1 + D_p Q^2),$$

$$\frac{Q^2}{4\pi e^2}v^2(Q) \sim \Omega_p^2\left(1 - \frac{(RQ)^2}{6}\right),$$

with the parameters D_p and R describing the ionic plasma dispersion at long wavelengths and an ion mean-square radius, respectively. The resulting dispersion, to be associated with the propagating longitudinal density fluctuation mode, is

$$\lim_{Q\to 0}\omega^2(Q) = \lim_{Q\to 0}\left[\frac{\Omega_p^2}{\epsilon(Q)} + \Omega_p^2\left(\frac{R^2}{6} + D_p\right)Q^2 + \mathcal{O}(Q^4)\right]$$
$$= \left(\frac{\Omega_p}{k_s}\right)^2 Q^2 + \Omega_p^2\left(\frac{R^2}{6} + D_p\right)Q^2,$$

which shows that, even when $\epsilon(Q)$ is not positive, $\omega^2(Q)$ is positive defined, and hence a real-valued dispersion $\omega(Q)$ exists, depending on the relative size of the term $[R^2/6 + D_p]$. The associated velocity is

$$c^2 = c_{BS}^2 + \Omega_p^2\left(\frac{R^2}{6} + D_p\right). \qquad (4)$$

To get an esitmate of the deviations of the velocity from the BS value, which are embodied in the $[R^2/6 + D_p]$ term, we applied Eq. (4) to the experimental data, inserting the measured values of the collective-mode velocity in the left-hand side of the equation and using for c_{BS}^2 the data calculated under the beyond-RPA scheme. The results for the $[R^2/6 + D_p]$ term are reported in the last column of Table I.

An inspection of Table I shows that systematic trends are present. First, there is a clear tendency within the alkali-metal series, where the low-atomic-mass elements Li and Na show a behavior different from that of the heavier companions K, Rb, and Cs, consistently with an overall increase of the ionic influence. Indeed, in the case of Li and Na the rather small contribution $[R^2/6+D_p]$ is consistent with the expected reduced size of the ion core radius. A larger ion contribution in K, Rb, Cs, and also the $K_{52}Cs_{48}$ alloy is responsible for the *right* behavior of the collective-mode velocity, because of the small contribution of the electron gas term $(\Omega_p/k_s)^2$. Interestingly, rather small core contributions are associated to the *sp*-like metals Ga, Ge, Sn, Hg, and Pb. Even though less remarkable than in heavy alkali metals, ion core effects must be taken into account to correctly describe the dynamics of *sp*-like polyvalent metals, as also suggested by the present MD simulation.

As to the mode damping, a rather uninfluential temperature dependence, possibly a small decrease, of the collective-mode damping was observed. Were the damping of the collective mode due to its interaction with the whole of the ion dynamics, an increase of the damping with the temperature would have been observed. On the contrary, given the consistently large difference between the two temperatures here investigated, together with the almost constant experimental damping, it is rather straightforward to conclude that the attenuation of the ion-density fluctuations is primarily due to the interaction with the conduction electrons. Since electron states are expected to be almost temperature independent, at least over the present scale, no temperature dependence of the transition rate associated with the interaction between the collective mode and the electron system is expected. Indeed, from the calculated electron density at 320 K a Fermi energy equal to 9.7 eV is obtained in Ga, which corresponds to a Fermi temperature in excess of 10^5 K, against which the temperatures of the present experiment are definitively negligible. It is interesting to observe that a similar behavior is reported for liquid Sn,[28] where almost no temperature dependence of $\Gamma_c(Q)$ was observed. These results, although not conclusive, suggest that investigating the damping of the collective modes in metals could be an interesting and alternative approach to the study of the electron-mediated interactions.

As a final remark we note that the whole set of the results of Table I suggests that the electron contribution is critical for a proper treatment of the collective-mode velocity, that beyond-RPA approaches in conjunction with the most accurate data on the correlation energy have to be applied, and that a more sophisticated modeling of the ion contribution, instead of the simple empirical $[R^2/6+D_p]$, is mandatory.

ACKNOWLEDGMENTS

We wish to acknowledge the support of Marco Sampoli in providing the MD code and offering his valuable help in getting one of us (L.E.B.) trained in the use of the code.

[1] J. R. D. Copley and J. M. Rowe, Phys. Rev. Lett. **32**, 49 (1974); T. Bodensteiner, Chr. Morkel, W. Gläser, and B. Dorner, Phys. Rev. A **45**, 5709 (1992); P. Verkerk, P. H. K. de Jong, M. Arai, S. M. Bennington, W. S. Howells, and A. D. Taylor, Physica B **180-181**, 834 (1992); F. J. Bermejo, M. L. Saboungi, D. L. Price, M. Alvarez, B. Roessli, C. Cabrillo, and A. Ivanov, Phys. Rev. Lett. **85**, 106 (2000); C. Cabrillo, F. J. Bermejo, M. Alvarez, P. Verkerk, A. Maira-Vidal, S. M. Bennington, and D. Martin, *ibid.* **89**, 075508 (2002).

[2] O. Soderstrom, J. R. D. Copley, J.-B. Suck, and B. Dorner, J. Phys. F: Met. Phys. **10**, L151 (1980).

[3] L. E. Bove, F. Sacchetti, C. Petrillo, and B. Dorner, Phys. Rev. Lett. **85**, 5352 (2000).

[4] L. E. Bove, F. Sacchetti, C. Petrillo, B. Dorner, F. Formisano, and F. Barocchi, Phys. Rev. Lett. **87**, 215504 (2001).

[5] L. E. Bove, B. Dorner, C. Petrillo, F. Sacchetti, and J.-B. Suck, Phys. Rev. B **68**, 024208 (2003).

[6] H. Sinn, F. Sette, U. Bergmann, Ch. Halcoussis, M. Krisch, R. Verbeni, and E. Burkel, Phys. Rev. Lett. **78**, 1715 (1997); T. Scopigno, U. Balucani, G. Ruocco, and F. Sette, *ibid.* **85**, 4076 (2000); Phys. Rev. E **63**, 011210 (2001); **65**, 031205 (2002).

[7] U. Balucani, A. Torcini, and R. Vallauri, Phys. Rev. A **46**, 2159 (1992); Phys. Rev. B **47**, 3011 (1993); M. Canales, L. E. Gonzalez, and J. A. Padro, Phys. Rev. E **50**, 3656 (1994); A. Torcini, U. Balucani, P. H. K. de Jong, and P. Verkerk, *ibid.* **51**, 3126 (1995).

[8] L. E. Bove, F. Sacchetti, C. Petrillo, B. Dorner, F. Formisano, F. Barocchi, and M. Sampoli, Philos. Mag. B **82**, 265 (2002); J. Non-Cryst. Solids **307–310**, 842 (2002).

[9] U. Bafile, P. Verkerk, F. Barocchi, L. A. de Graaf, J. B. Suck, and H. Mutka, Phys. Rev. Lett. **65**, 2394 (1990); A. Cunsolo, G. Pratesi, G. Ruocco, M. Sampoli, F. Sette, R. Verbeni, F. Barocchi, M. Krisch, C. Masciovecchio, and M. Nardone, *ibid.* **80**, 3515 (1998); A. A. van Well and L. A. de Graaf, Phys. Rev. A **32**, 2396 (1985).

[10] J. M. Holender, M. J. Gillan, M. C. Payne, and A. D. Simpson, Phys. Rev. B **52**, 967 (1995); J. Hafner and J. Kahl, J. Phys. F: Met. Phys. **14**, 2259 (1984); J. Hafner and W. Jank, Phys. Rev. B **42**, 11 530 (1990).

[11] M. C. Bellissent-Funel, P. Chieux, D. Levesque, and J. J. Weis, Phys. Rev. A **39**, 6310 (1989).

[12] X. G. Gong, G. L. Chiarotti, M. Parrinello, and E. Tosatti, Phys. Rev. B **43**, 14 277 (1991); Europhys. Lett. **21**, 469 (1993).

[13] F. J. Bermejo, M. Garcia-Hernandez, J. L. Martinez, and B. Hennion, Phys. Rev. E **49**, 3133 (1994).

[14] F. J. Bermejo, R. Fernandez-Perea, M. Alvarez, B. Roessli, H. E. Fischer, and J. Bossy, Phys. Rev. E **56**, 3358 (1997).

[15] T. Scopigno, A. Filipponi, M. Krisch, G. Monaco, G. Ruocco, and F. Sette, Phys. Rev. Lett. **89**, 255506 (2002).

[16] M. Inui, S. Takeda, and T. Uechi, J. Phys. Soc. Jpn. **61**, 3203 (1992).

[17] C. Petrillo, F. Sacchetti, B. Dorner, and J.-B. Suck, Phys. Rev. E **62**, 3611 (1999); F. Sacchetti, J.-B. Suck, C. Petrillo, and B. Dorner, *ibid.* **69**, 061203 (2004).

[18] M. J. Cooper and R. Nathans, Acta Crystallogr. **23**, 357 (1967); B. Dorner, Acta Crystallogr., Sect. A: Cryst. Phys., Diffr., Theor. Gen. Crystallogr. **28**, 319 (1972).
[19] K. Sköld, and D. L. Price, *Neutron Scattering*, Methods of Experimental Physics, Vol. 23A (1986), p. 536.
[20] C. Petrillo and F. Sacchetti, Acta Crystallogr., Sect. A: Found. Crystallogr. **46**, 440 (1990).
[21] J. G. Dil and E. M. Brody, Phys. Rev. B **14**, 5218 (1976).
[22] J. Friedel, Philos. Mag. **43**, 153 (1953).
[23] *Handbook of Chemistry and Physics*, 79th ed. (CRC Press, Boca Raton, 1999).
[24] P. D. Welch, IEEE Trans. Audio Electroacoust. **AU-15**, 70 (1967).
[25] L. E. Bove, F. Sacchetti, C. Petrillo, F. Formisano, M. Sampoli, and F. Barocchi, Philos. Mag. **84**, 1609 (2004).
[26] N. H. March, *Liquid Metals* (Cambridge University Press, Cambridge, England, 1990).
[27] U. Balucani and M. Zoppi, *Dynamics of the Liquid State* (Clarendon Press, Oxford, 1994).
[28] S. Hosokawa, J. Greif, F. Demmel, and W.-C. Pilgrim, Chem. Phys. **292**, 253 (2003).
[29] S. Hosokawa, Y. Kawakita, W.-C. Pilgrim, and H. Sinn, Phys. Rev. B **63**, 134205 (2001).
[30] D. Pines, and Ph. Nozieres, *The Theory of Quantum Liquids* (Benjamin, New York, 1966); D. Pines, *Elementary Excitations in Solids* (Benjamin, New York, 1963).
[31] N. Iwamoto, Phys. Rev. A **30**, 3289 (1984).
[32] P. Gori-Giorgi, F. Sacchetti, and G. B. Bachelet, Phys. Rev. B **61**, 7353 (2000).
[33] F. Sacchetti, E. Guarini, C. Petrillo, L. E. Bove, B. Dorner, F. Demmel, and F. Barocchi, Phys. Rev. B **67**, 014207 (2003).